

The Effect of Ladder-Bar Shape Variation for A Ladder-Secondary Double-Sided Linear Induction Motor (LSDSLIM) Design to Cogging Force and Useful Thrust Performances

Mochammad Rusli^{1,2}, I. N. G. Wardana², Moch Agus Choiron² and Muhammad Aziz Muslim¹

¹Electrical Engineering Dept., Faculty of Engineering Brawijaya University, Malang, INDONESIA

²Mechanical Engineering Dept., Faculty of Engineering Brawijaya University, Malang, INDONESIA
rusli@ub.ac.id

Abstract—This paper describes an investigation on the variation of the magnetic circuit of LSDSLIM (Ladder Secondary Double-Sided Linear Induction Motors) for the ladder-bar shape effects of cogging action and useful thrust. The comparisons are based on the Maxwell Stress method and FE method. The background of this investigation is related to that there are conflicts between the air gap length and cogging force and useful thrust for the Linear induction motor design with ladder secondary. Therefore, as the first stage of the design, the objectives are to investigate the minimum cogging forces and maximum useful thrust for the ladder shape effect. The methodology of investigation is based on the variation of the tooth width and the slot width of stationary part for the variation of the shape of ladder-bars. The tooth width and the slot width of moving part remain constant. The two ladder-shaped which are investigated include trapezoidal ladder bar and rectangular ladder bar. In each shape, the variation of the ratio between the tooth width and the slot width of ladder bar is conducted, and the maximum magnitude of the cogging action and magnitude maximum of useful thrust are investigated. The goodness of this procedure is the ratio between cogging action to useful thrust. This investigation shows that the trapezoid-Ladder Bars can decrease the magnitude of the Cogging Action in linear induction motor until 2.5% compared to the rectangular ladder-bars, and the thrust does not decrease in significant value.

Index Terms—Ladder Secondary Double-Sided Linear Induction Motor; Electromagnetic Field; Cogging Force.

I. INTRODUCTION

This paper describes the essential requirement in designing a double-sided linear induction motor with ladder secondary (LSDSLIM). In the design process, a relationship between the three-phase current source with the distribution magnetic flux density in the air gap plays an important role. As a linear motor moves, the real air gap length varies, which can cause the variation of the relationship between the magnetic flux with the current source. The secondary ladder-bars shape of LSDSLIM influences the variation of distribution magnetic flux density. It can also generate the cogging action that can produce an unprecise movement of the motor.

The linear induction motors have some advantages over its rotary induction motor. The linear induction motor has less friction and no backlash when compared to the rotary induction motor. It results in a high precision movement, and there are no mechanical limitations, especially on the

acceleration and velocity. The velocity is constrained only by the bandwidth of the position measurement system, especially on an encoder device, or by the power electronics. The linear motor has higher reliability and longer lifetime, due to mechanical simplicity [1].

The ladder bar shape variation will be investigated in this paper concerning the cogging action and useful thrust. The aim is to obtain some data for the ladder-bar shape variation effects over cogging action and useful thrust [2]. It also provides views of different ladder shapes which can influence the motor performance. This paper describes just two critical aspects: reducing cogging action (tangential forces) and maintaining the useful thrust that aims for improving the precision of the linear feed axes in machine tools. The investigation process proposed in this study focuses on the impact of the geometrical dimensions of the physical motor on cogging action and useful thrust.

The other reason for this investigation is that there are some conflicts between the magnitude of the cogging action and useful thrust [3]. To obtain more significant useful thrust, the air gap length should be smaller. However, it can lead to the magnitude of cogging action to increase significantly. It is caused by the cogging action and useful thrust which depend strongly on the air gap length and shape of the secondary-ladder shape of the magnetic circuit in linear induction motors [4]. Therefore, as the first stage of design for objectives minimum cogging action and maximum useful thrust is the effect of ladder shape should be investigated. So, it can contribute to the LIM design with minimum cogging action or the improvement of precision movement level.

The trapezoidal ladder-bar in this paper will be investigated by comparing with the rectangular ladder-bar. The reason is that the trapezoidal ladder bar can reduce the tangential force (cogging action). It can be explained by the Maxwell stress concept. If the magnetic field is perpendicular to the surface of a body, there will be the magnitude of tensile stress also perpendicular to the surface of the field. If the field is parallel to the surface, there will be the magnitude of compressive stress pushing the surface out of the field. The surface of trapezoidal can reduce the number of magnetic field path where are perpendicular to the surface of the iron core. Because the surface-side of trapezoidal shape is not a straight line, but an oblique line, therefore there is a possibility for reducing the magnetic forces between tooth in LSDSLIM with ladder secondary.

II. THE RECTANGULAR BAR EFFECTS ON COGGING ACTION

The relationship between the air gap length and the cogging action can be described by the energy magnetic variation in the air gap [5]. A linear induction motor can be referred to the existence of cogging forces in an LSDSLIM. The forces can be detected by energy variation or the magnetic energy gradient in both air gap, which can be described mathematically as the derivative of energy:

$$F_c = \frac{2\mu_0}{g_e} \frac{d}{dx} \left[\int_0^{\tau} B^2(x) dx \right] \quad (1)$$

where:

F_c : Cogging Force

μ_0 : Permeability of the air gap

g_e : The air gap length equivalent

The Equation (1) shows that the cogging forces depend strongly on the air gap length equivalent. If the air gap length equivalent is smaller, the cogging forces increase significantly. The following paragraph will describe the derivation of the air gap length equivalent to rectangular bars.

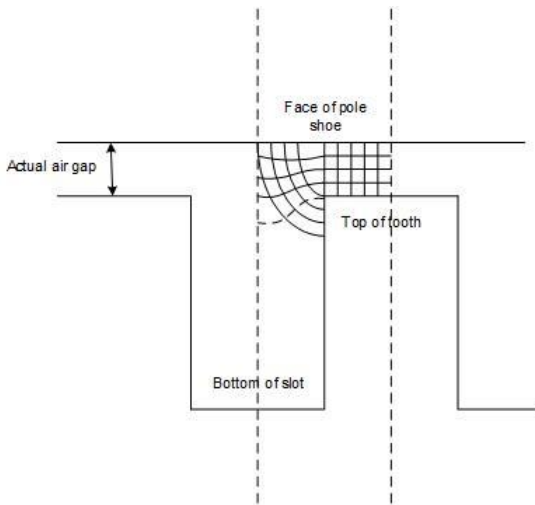


Figure 1: Magnetic Flux Between Pole Face and Rectangular Bar Shape

The magnetic field lines in between un-slotted pole face to the slotted core are shown in Figure 1. Figure 1 describes a correct magnetic flux plot entering the tops and sides of the core tooth and slot. This takes no account of magnetic saturation the iron, but the assumption of very high permeability of the iron is justified since the flux density is usually is comparatively low near the top of the tooth. To explain how the reluctance of the air paths between pole face and slotted core may be calculated, the magnetic line is approximated to follow the paths as indicated in Figure 2.

The correct magnetic flux as shown in Figure 1 is approximated as shown in Figure 2. The magnetic flux lines from the surface of up-side are supposed to follow a path consisting of a straight line of air gap length g , and then a circular path with a radius of r . All approximated correct magnetic lines are indicated in Figure 2. This is apparently a

simple assumption, but it is convenient for calculation and provides very good results.

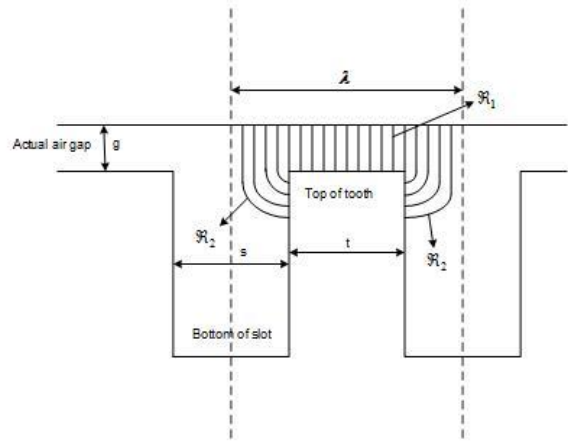


Figure 2: Approximate Shape of The Magnetic Flux Path

If a part of the air gap is 1 mm long axially (i.e. in a direction normal to the plane of the section shown in Figure 2) and the reluctance over the slot pitch is made up of two parts: the reluctance between the pole face and top of tooth:

$$\mathfrak{R}_1 = \frac{g}{\mu_0 A} = \frac{1}{P_1} \quad (2)$$

Where:

g : The reel air gap length

P_1 : Permeance between surface and tooth

μ_0 : The permeability of the air gap

A : The Distance between tooth in the moving and stationary part.

In this case, the permeability of the air gap is 1; so, the Equation (1) can be simplified into:

$$\mathfrak{R}_1 = \frac{g}{w_t} \quad (3)$$

Moreover, the reluctance of $2 \mathfrak{R}_2$ where \mathfrak{R}_2 is the reluctance between the pole face and one middle of the tooth. The reluctance of any small section of thickness (dr) and depth 1 mm measured as shown in Figure 2, is:

$$d\mathfrak{R}_2 = \frac{g + (\pi r/2)}{dr} \quad (4)$$

Equation (3) can be used for the calculation of reluctance number 2. In the left of equal sign can be solved by the integration of both sides in a limited range between 0 until half of slot $s/2$. The fundamental process would be easier if integral of the reciprocal of reluctance which is called as the permeance:

$$\int_0^{\pi/2} d\left(\frac{1}{\mathfrak{R}_2}\right) = \int_0^{\pi/2} dP_2 = \int_0^{\pi/2} \frac{dr}{g + (\pi r/2)} \quad (5)$$

Where:

- P_2 : Permeance between the pole face to the middle of the slot
- g : The actual air gap
- s : Slot
- r : radius of circular field paths

Whence:

$$P_2 = \frac{\pi}{2} \int_0^{\frac{s}{2}} \frac{dr}{(2g/\pi) + r} = \frac{\pi}{2} \ln \left(\frac{g + (\pi s/4)}{g} \right) \quad (6)$$

The average permeance per square millimeter (mm^2) over the tooth pitch at the centre of the pole is:

$$P_{total} = \frac{P_1 + 2P_2}{\lambda} = \frac{\frac{t}{g} + 4\pi \ln \left(\frac{\pi s}{4g + 1} \right)}{\lambda} \quad (7)$$

where the tooth pitch λ is expressed in millimetres (mm). The reciprocal of the permeance is the reluctance \mathfrak{R} per square millimetre of the air gap cross-section for an average length, or what may be called an equivalent air gap length (EAGL), equal to g_e . Since $\mathfrak{R} = l/A$, and $A=1 \text{ mm}^2$, so the equivalent air gap length is:

$$g_e = \frac{\lambda}{\frac{t}{g} + \frac{4}{\pi} \ln \left(\frac{\pi s}{4g} + 1 \right)} \quad (8)$$

Based on Equation (8), the air gap equivalent depends strongly on the width of slot and tooth. Because the cogging force depends on the air gap length equivalent (Equation (1)), so reducing the cogging force can be done by changing the ladder-bar shape. Using the finite element method (FEM), the comparison of the magnitude of the cogging force and useful thrust between rectangular ladder bar shape with the trapezoidal ladder bar shape is conducted for a double-sided linear induction motor drive.

III. FEM ANALYSIS OF THE RECTANGULAR-LADDER BARS

Currently, FEM is used mostly in solving the similar air gap length problems. It is because FEM provides the high capabilities and ability to provide the precision results. This method consists of the design of the geometry of the model, defining the material types of different parts of the model and its parameters and physical characteristics. Each surface of the model is meshed by elements suitable for the required analysis.

The rectangular ladder-bar shape of LIM-model is investigated. The geometric parameters of moving part based on the MEC approximation predicted in the previous section. This model is the open tooth model which has the rectangular ladder bar. The height of the ladder is 5 mm length. Using the Flux software, the model is simulated. The volume of ladder-bars is not be changed. The current and the number turns of

the coil are constant. The geometrical dimensions of moving part are also constant. The tooth width of stationary part is varied in a range between 6 mm to 20 mm.

The maximum flux density in this model is 0.890. The flux density distribution in the magnetic moving core and the stationary magnetic core is under 0.89 Tesla. The coils have been supplied by the constant three phases electrical current with the frequency of 50 Hz and the primary parts have been moved by a constant speed of 3.5 m/s. Based on the pole pitch 50 mm in the frequency of the input signal, the synchronous speed is 5 m/s. The slip of model was $s=0.3$.

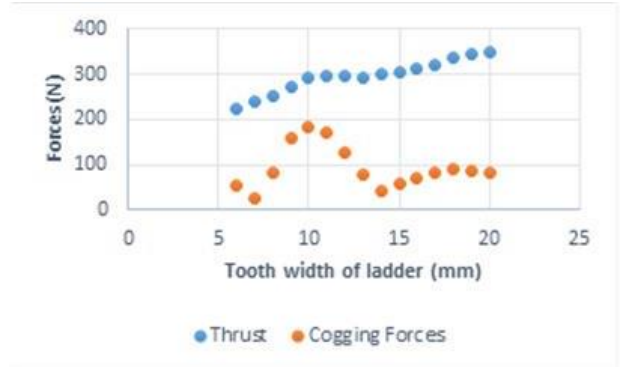


Figure 3: The cogging and thrust magnitude for tooth width variation

Figure 3 describes the relationship between tooth width variation and the cogging forces and useful thrust. The increase of useful thrust is proportional directly to increasing the tooth width. However, cogging force is proportional to the ratio between the tooth width of the primary and secondary layer. The cogging maximum will happen as the ratio of them is one or both of them have the similar width. It is caused by the reluctance of air gap of the model in this size is of minimal value when the surface of both tooth is opposite each other. Therefore, the gradient of stored magnetic energy (cogging force) in air gap might be more significant.

Figure 3 shows that cogging forces decrease in about 10. However, the useful thrust also decreases until about 30. Even though the cogging force is decreased until under 10 N, the useful thrust also decreases until 210 N. In other to get the minimum cogging forces and the useful thrust is not decreased significantly, the one alternative model is the ladder-bars of the stationary should be changed into the trapezoidal ladder-shape one.

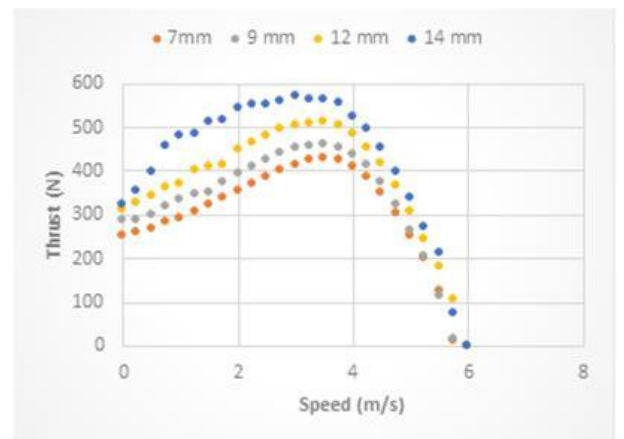


Figure 4: Thrust-Speed Characteristic for rectangular Ladder-Bars

Figure 4 shows the steady-state characteristic of LDSLIM with the variation of tooth width of ladder-bars. With the increasing of the ladder-bar width, the maximum thrust increases significantly. However, in very low-speed conditions, the thrust is not changed significantly. It shows that the ladder-bar width variation contributes significantly to the increase of useful thrust.

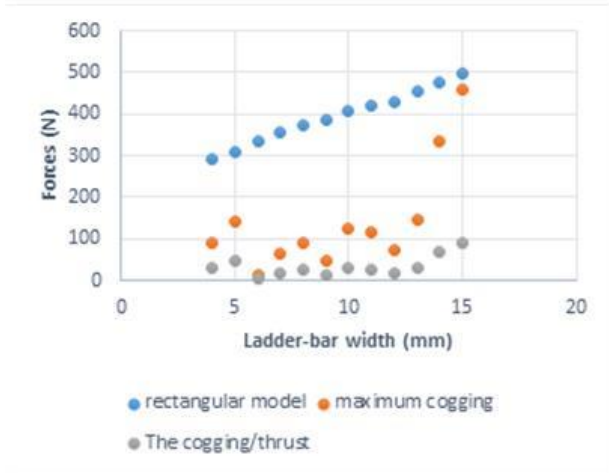


Figure 5: Cogging and Thrust Ratio for Rectangular Ladder-Bars

For the rectangular model by the ladder-bar width variation, cogging action could not be reduced until under 10%. The cogging action value is under 10 % occurred only as the tooth width is 6 mm. Table 1 shows all of the simulation results of cogging action measurement and percent to the useful thrust. Figure 5 shows the comparison between thrust and cogging forces for the rectangular model.

Table 1
Cogging and Thrust Ratio for Rectangular-Bars

t-width (mm)	Cogging (N)	Thrust	Percent cogging (%)
4	89.4	291.36	30.6836903
5	143.28	309.28	46.3269529
6	12.92	334.12	3.86687418
7	63.68	355.76	17.8997077
8	90.92	373.72	24.3283742
9	49.2	386	12.746114
10	126.56	406.52	31.1325396
11	115.48	418.68	27.5819241
12	74.6	429	17.3892774
13	145.92	454.56	32.1013728
14	333.12	478.32	69.6437531
15	457.2	499.48	91.5351966

IV. FEM ANALYSIS OF TRAPEZOIDAL-LADDER BARS

The following model is a trapezoidal-ladder bar shape DSLIM-model. The cross-section of the ladder is formed in a trapezoidal shape. This shape has two sides with different length, a long and a short side. Figure 4 shows a trapezoidal ladder-bar. The impact of the variation of the short side to the magnitude of cogging forces is firstly investigated.

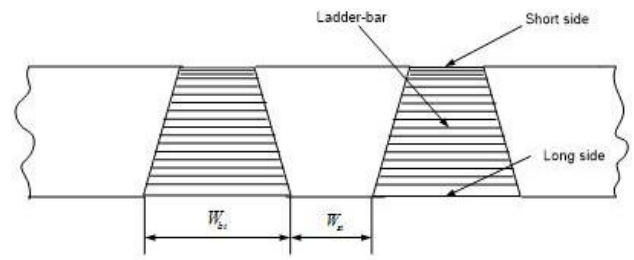


Figure 6: Trapezoidal Ladder-Bars

Then the ratio between long side of trapezoidal ladder-bar (W_{bt}) and core between ladder-bar (W_{st}) is varied. The height of ladder-bar and dimensions of the moving part remains constant. The geometrical dimensions of moving part remain constant. The Ampere-turn of coils is also unchanged.

A proposed LDSLIM-with trapezoidal ladder-bar is shown in Figure 6. The difference of this model to the LDSLIM with rectangular ladder-bar lies in the ladder-bar shape. In this model, the non-magnetic material bars are formed in a trapezoidal shape. One of the parameters that has an impact on the magnitude of the cogging forces is the short side of ladder-bar. A great significant impact on the magnitude of cogging forces is the ratio between ladder-bar width to the magnetic stationary core width.

Principally, the trapezoidal ladder bar can reduce the tangential force. It can be explained by the Maxwell stress concept. If the magnetic field is perpendicular to the surface of a body, there will be the magnitude of tensile stress $-B^2/\mu_0$ also perpendicular to the surface, drawing the surface into the field. If the field is parallel to the surface, there will be the magnitude of compressive stress pushing the surface out of the field. The surface of trapezoidal can reduce the number of magnetic field path where are perpendicular to the surface of the iron core. Therefore there is a possibility of reducing the magnetic forces between tooth in motor

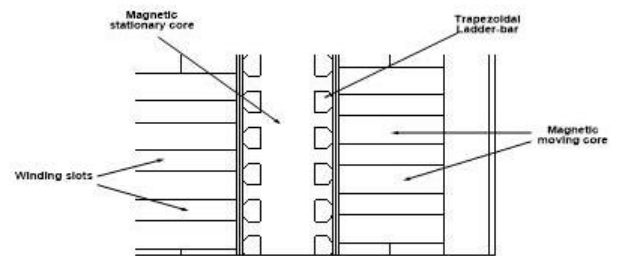


Figure 7: LDSLIM with Trapezoidal Ladder-Bars

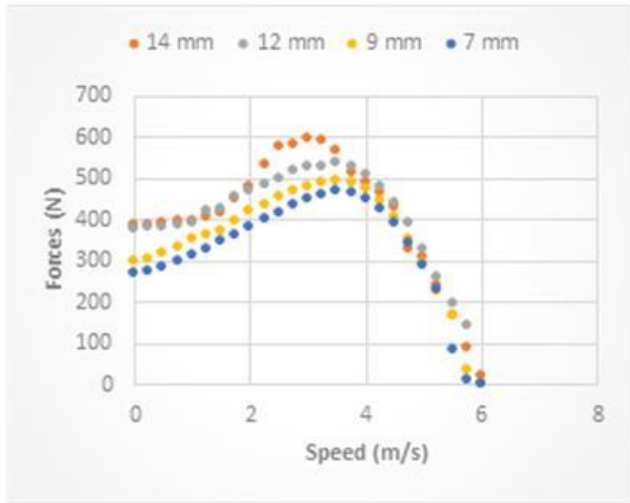


Figure 8: Thrust-Speed Characteristic of the Trapezoidal Ladder-Bars

The trapezoid ladder-bar model can lead to the decreasing of the magnitude of cogging forces. The useful forces remain unchanged. The optimisation process involves the variation of the short sides of trapezoidal ladder-bar, the variation of tooth width of the trapezoidal ladder-bar in the range between 4 – 15 mm by steps in 1 mm length.

The variation of short sides shows that the short side of 3 mm, the motor has minimum cogging forces. The following paragraph shows the results of the variation of tooth width of stationary part. Figure 8 shows the relationship between the thrust and speed of the trapezoid ladder-bar model. The tooth width variation can change the steady state characteristic of the model. The critically slip are not influenced by the tooth width variation (see Table 2). The increasing of the tooth width causes the increasing of the maximum thrust of the motor.

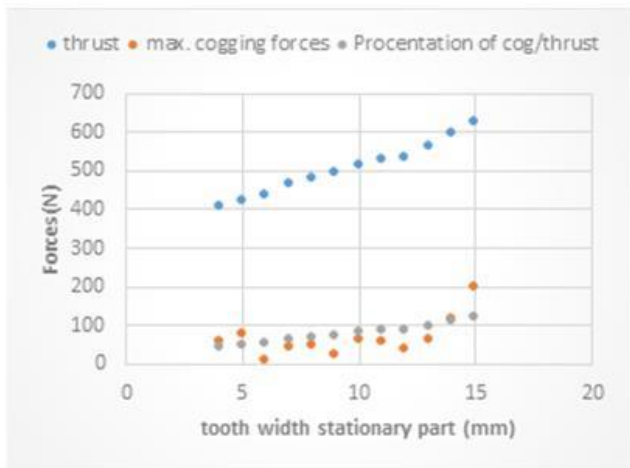


Figure 9: Cogging and Thrust Ratio for Trapezoidal Ladder-Bars

Table 2 shows the useful thrust of the trapezoidal ladder-bar model. Compared to the rectangular model, the maximum cogging forces can reach the percent of 31.17. However there is three tooth width have the cogging force under 10: 6 mm, 7 mm, 9 mm, and 12 mm tooth width. It means that the trapezoidal shape can reduce the cogging forces significantly and the useful thrust is not changed significantly.

Table 2
Cogging and Thrust

Tooth Width (mm)	Max Thrust (N)	Critical Slip
4	407.63598	0.45
5	422.07696	0.42
6	437.90008	0.45
7	466.78204	0.42
8	479.74556	0.42
9	492.66142	0.42
10	513.01224	0.45
11	526.30938	0.42
12	534.93584	0.42
13	564.43738	0.5
14	596.60788	0.5
15	625.39452	0.5

Table 3 shows that the trapezoidal ladder-bar model can maintain the magnitude of the useful thrust and reduce the cogging forces for tooth-width 9 mm length. The useful thrust increases when the tooth width of ladder-bar also increases. However, the cogging forces do not always increase when the tooth width is increased. Only in the certainty tooth width, the ratio between cogging forces and tooth width is smaller. The smallest ratio between cogging forces and useful thrust is tooth width of ladder-bar is 6 mm length.

Table 3
Cogging and Thrust Ratio

T-Width (mm)	Cogging (N)	Thrust	Percent. Cogging (%)
4	57.192	407.636	14.03016485
5	75.73174	422.077	17.94263776
6	10.38988	437.9001	2.372659991
7	40.70164	466.782	8.71962426
8	48.3749	479.7456	10.08344924
9	12.29628	492.6614	2.495888556
10	59.90862	513.0122	11.67781494
11	58.6218	526.3094	11.13827764
12	39.03354	534.9358	7.296863863
13	59.47968	564.4374	10.53787047
14	113.9551	596.6079	19.10049529
15	198.6945	625.3945	31.77107148

The comparison of the useful thrust and the cogging forces for both models, trapezoidal and rectangular ladder-bar is investigated. On each tooth width, the cogging action and useful thrust are measured using Flux-Cedrat and compared. The results of the comparison are plotted into the curves shown in Figure 8. All cogging actions generated in trapezoidal ladder-bar are smaller than in the rectangular ladder-bar. For each variation of tooth width, the thrust measured show that thrust produced by the trapezoidal ladder-bar model is more significant than by the rectangular ladder-bar.

V. CONCLUSION

The rectangular Ladder-bars in the stationary part of LSDSLIM-Model cannot reject the magnitude of Cogging Action significantly. With tooth and slot width ratio variation, it can only reduce the ratio of the magnitude of the cogging action and thrust about 12 %. However, with the trapezoidal Ladder-Bars, the cogging force can be pushed until Cogging/thrust is 2.5 %.

ACKNOWLEDGEMENT

The authors would like to thank the High Educational Directorate of the National Education Ministerium of the Republic of Indonesia for financially supporting this project.

REFERENCES

- [1] Alger, P. L. 1970. *Induction Machines*, New York, Gordon and Breach, Science Publisher, Inc.
- [2] Rusli, M., "Reducing Cogging Force in A Cage-secondary Linear Induction Motor (LIM) by One-Side Shifting", 2012, *The 6th – Electrical Power, Electronics, Communications, and Informatics International Seminar 2012*, Malang.
- [3] Brueckel, S. 1999. "Feed-Drive System with a Permanent Magnet Linear Motor for Ultra Precision Machine Tools". *IEEE 1999 International Conference on Power Electronic and drive System*.
- [4] Rusli, M., Moscrop, J., Platt, D., Cook, C. 2011. An Analytical Method for predicting Cogging Forces in Linear Induction motors. *LDIA 2011*.
- [5] Kok Kiong Tan, Hui Fang Doi, Yang quan Chen and Tong Heng Lee, "High Precision Linear Motor Control Via Relay-Tuning and Iterative Learning Based on Zero-Phase Filtering", *IEEE Transactions on Control Systems Technology*, Vol. 9, No. 2, pp. 244-253, March, 2001.